Article:

Angelopoulou, D., Meunier, V., Forny, L. et al. (3 more authors) (2021) Influence of localized thermal effects on the reconstitution kinetics of lactose-coated whole milk powder. Food Research International, 150 (Part A). 110774. ISSN 0963-9969

https://doi.org/10.1016/j.foodres.2021.110774

Influence of localized thermal effects on the reconstitution kinetics of lactose-coated whole milk powder

Diamanto Angelopoulou[1], Vincent Meunier[2], Laurent Forny[3], Gerhard Niederreiter[2], Stefan Palzer[4], Agba D. Salman[1]

[1] Department of Chemical and Biological Engineering, University of Sheffield, S1 3JD Sheffield, UK

[2] Nestlé Research, Vers-chez-les-blanc, 1000 Lausanne 26, Switzerland

[3] Nestlé Product Technology Center, Route de Chavornay 3, 1350 Orbe, Switzerland

[4] Nestlé SA, Avenue Nestlé 55, 1800 Vevey, Switzerland

*

Abstract

Reconstitution of dairy powders is strongly influenced by the presence and physical state of fat on the particle surface. The present study investigates the effect of a micronized lactose coating on the physical state of the fat and the reconstitution kinetics of whole milk powder at four different temperatures (4/21/40/60°C) and two stirring rates (400/800 rpm). For this purpose, two types of micronized lactose were used as coating materials: crystalline and amorphous.

At 4°C and 21°C, the coated powders sink and are reconstituted faster than pure whole milk powder, regardless of the stirring rate applied. At 40/60°C and 400 rpm, although the amorphous micronized lactose coating leads to a significant decrease in the reconstitution time, the crystalline coating has the opposite effect (or no effect). This discrepancy is related to the large differences in terms of dissolution enthalpy between the two micronized lactose physical states. It is posited that the dissolution of the coating material causes a temperature shift at the powder-water interface which could hamper the complete melting of surface fat and influence its viscosity, thereby affecting wetting

---

[*] Abbreviations: ML, Micronized Lactose; SMP, Skimmed Milk Powder; WMP, Whole Milk Powder

and sinking. These differences are overcome at a high stirring rate (800 rpm) or if agglomerated whole milk powder is used as the host material.

Keywords

Enthalpy; Amorphous; Crystalline; Particle surface; Wetting; Dissolution; Rehydration

1 Introduction

In spray-dried dairy powders, a disproportionately high concentration of fat is typically observed on the particle surface in comparison to the bulk (Foerster et al., 2016; Gaiani et al., 2006; Kim et al., 2009; Murrieta-Pazos et al., 2012; Nijdam & Langrish, 2006). Milk fat is made of a mixture of triacylglycerols, with different melting points depending on the type of esterified fatty acids (i.e. unsaturated/saturated, molecular weight). As a result, the melting of milk fat occurs within a wide range of temperatures (Kim et al., 2005).

The melting characteristics of surface fat have been associated with important functional properties of the powder. One such property is the reconstitution. Powder reconstitution occurs in four physical steps: wetting, sinking, dispersion and dissolution (Mitchell et al., 2015). Wetting is the first step of powder reconstitution, during which the liquid is brought into contact with the powder and penetrates the intra- and interparticle pores of the bed, driven by capillary forces (Forny et al., 2011; Mitchell et al., 2015). Sinking is the second step of powder reconstitution, when the powder gets submerged into the liquid (Mitchell et al., 2019). Dispersion is the break-up of agglomerates and aggregates (lumps) into smaller aggregates or primary particles (Forny et al., 2011; Mitchell et al., 2020). Lastly, dissolution occurs when the two phases (solid and liquid) form a homogeneous phase, i.e. the solution (McNaught & Wilkinson, 1997).

Kim et al. (2005) reported that the static sinking time of whole milk powder (WMP) is > 15 min when the water temperature is between 10°C and ~ 37 °C, i.e. if the surface fat is partially solid. Above 38°C, where the surface fat is expected to be fully liquid, a sharp decrease is observed in terms of sinking time. This suggests that the reconstitution behavior of fat-based powders is largely dependent on the physical state of surface fat. Similar observations have been reported by Mitchell et al. (2020).

In the present study, the surface of WMP is modified by the deposition of micronized lactose (ML) particles via dry coating. In dry particle coating, fine (guest) particles are attached to the surface of relatively large (host) particles, driven by attractive interparticle forces (van der Waals and/or electrostatic) (Pfeffer et al., 2001; Saleh & Guigon, 2007). The guest particles are brought into contact with the host particles using mixing (Alonso et al., 1989).

Lactose is a material that can exist in both the amorphous and crystalline solid forms (Roos, 2010; Clark et al., 2016). α-Lactose monohydrate is the most stable form of crystalline lactose and is characterized by an endothermic dissolution (Harjunen et al., 2004; Huppertz & Gazi, 2016; Listiohadi et al., 2009). In contrast, amorphous lactose is unstable and dissolves exothermically (Harjunen et al., 2004). Harjunen et al. (2004) reported a linear relationship between the amorphous content of solid lactose and its enthalpy of dissolution, with increasing amorphous content leading to higher exothermicity. In multicomponent food powder systems containing lactose, such as dairy powders, the physical solid state of lactose influences the thermodynamic response of the powder during reconstitution. Marabi et al. (2007) studied the enthalpy of dissolution of skimmed milk powder (SMP) in the fully amorphous state and upon conditioning at 54% relative humidity, where most of the lactose had crystallized, and reported that crystallization causes a significant decrease in the exothermicity of SMP.

The objective of the present study is to investigate the effect of dissolution enthalpy of a crystalline vs. amorphous micronized lactose coating on the physical state and viscosity of surface fat during reconstitution at a wide range of temperatures. Ultimately, the objective is to understand how the enthalpy of dissolution of the coating material influences the reconstitution kinetics of coated fat-based powders.

2 Materials and Methods

2.1 Materials

The host powders used in this study were WMP from LacPatrick Dairies, Ireland (a_w = 0.24 at 20°C), agglomerated WMP from Nestlé Research, Switzerland (a_w = 0.13 at 20°C), and SMP from Emmi, Switzerland (a_w = 0.25 at 20°C).

The coating materials were micronized α-lactose monohydrate (from DFE Pharma, Netherlands) and micronized spray-dried lactose. The latter was prepared by spray drying an aqueous lactose solution (20% w/w, 70°C) in a Mobile Minor spray dryer (GEA, Denmark). The flow rate of the drying gas was ~ 100 kg/h. The inlet and outlet temperatures were 160°C and 90°C, respectively. Atomization was performed using a co-current two-fluid nozzle (1 mm orifice diameter) at 0.5 bar. The liquid flow rate was 4.5 kg/h. The spray-dried lactose powder was subsequently micronized using a J-70 jet mill (Tecnologia Meccanica, Italy). The micronized powder (a_w = 0.12 at 20°C) was stored in heat-sealed aluminum bags throughout the duration of the study to prevent moisture pickup that could induce caking and recrystallization.

The two micronized lactose powders were characterized using X-ray diffraction. X-ray diffraction was performed in a MiniFlex 600 (Rigaku, Japan). The measurement was conducted at a speed of 10°/min and a resolution of 0.02°. The X-ray source was copper (k-alpha 1.54 Å). Crystalline peaks were observed in the case of micronized α-lactose monohydrate, while micronized spray-dried lactose produced a broad hump with low intensities, typical of amorphous materials (data presented in Angelopoulou et al. (2021)). Therefore, the two powders are referred to in this study as crystalline micronized lactose (ML) and amorphous micronized lactose (ML), respectively.

2.2 Dry powder mixing

The host powder (WMP, agglomerated WMP or SMP) was mixed with the micronized lactose powder (crystalline or amorphous) in a high-shear mixer (Hotpoint 1000W, USA) equipped with a custom-made 45° pitched 3-blade impeller (20 cm diameter). The batch size of the mixture was 200 g and the concentration of micronized lactose in the mixture was 5% (w/w). For the agglomerated WMP mixture, an additional concentration of 3% (w/w) micronized lactose was tested. The mixing speed was set to 120 rpm for 5 min; These conditions were determined after preliminary experiments on the quality of mixing, showing neither breakage nor compaction phenomena.

2.3 Thermal imaging

The thermal effect as a result of the micronized lactose dissolution was determined using thermal (infrared) imaging. The thermal camera used was the A655sc model by Teledyne FLIR (Wilsonville, USA), which has a resolution of 640 x 480 pixels, detecting temperature differences down to < 30 mK, and accuracy of ± 2%. The frame rate was set to 50 fps.

For the thermal imaging experiments, powder beds of pure micronized lactose (crystalline or amorphous) were prepared by placing 2 g of powder in a glass petri dish (5 cm diameter). Apart from the micronized lactose powders, thermal imaging was also performed on layers of milk fat covered with micronized lactose. The fat layers were prepared by spin coating, using an L2001A3 spin coater by Ossila, UK; 1 ml of anhydrous milk fat (Emmi, Switzerland), heated at 70°C, was placed at the center of a microscope glass slide which was rotated at 1000 rpm for 60 s. The spin-coated slides were subsequently left at room conditions for at least 48 h. Afterwards, micronized lactose was sprinkled over the fat layer, and any excess material was removed.

The thermal imaging experiments involved the deposition of a deionized water droplet (4 µl, 20°C) on the surface of the sample using an electronic pipette (Xplorer, Eppendorf, Germany). Recordings were taken with the thermal camera placed from the top and were subsequently analyzed using the FLIR software (Teledyne FLIR, Wilsonville, USA). Optical video recordings were also taken using a digital microscope camera (AM-4013TL, Dino-Lite, Taiwan, 30 fps). The process was repeated ten times at each condition.

2.4 Reconstitution analysis

The custom-made reconstitution setup is presented in Figure 1. It consists of an unbaffled glass vessel containing deionized water (200 ± 0.1 ml), and a steel tube for feeding the powder (4 ± 0.01 g). The powder was introduced instantly to the liquid surface by opening the slide at the bottom of the feed tube (knife gate). Powder sinking was monitored using a video camera from the top (1920 x 1080 pixels, 30 fps). Powder dissolution was monitored using a conductivity probe placed vertically to the vessel (Jenway 3540 model, k value 0.111 cm^{-1} at 25 °C, UK). The water temperature was 4/21/40/60°C and the stirring rate was 400/800 rpm.

Stirring was performed using a magnetic stirring bar (cylindrical PTFE, 25 mm). This type of stirring creates a mixed flow pattern, with the contribution of tangential, axial and radial components (Bertrand et al., 2012; Obermayer et al., 2013). The average shear rate ($\dot{\gamma}$) corresponding to each impeller speed can be calculated using the Metzner and Otto equation (Metzner & Otto, 1957):

$$\dot{\gamma} = K \cdot N \tag{1}$$

where K is a nondimensional constant dependent on the type of impeller, and N is the shaft speed (revolutions per second). For a mixed flow pattern, the K value found in the literature is 5.4 (Wu et al., 2006). This gives a shear rate of 36 s^{-1} and 72 s^{-1} for a mixing speed of 400 and 800 rpm, respectively.

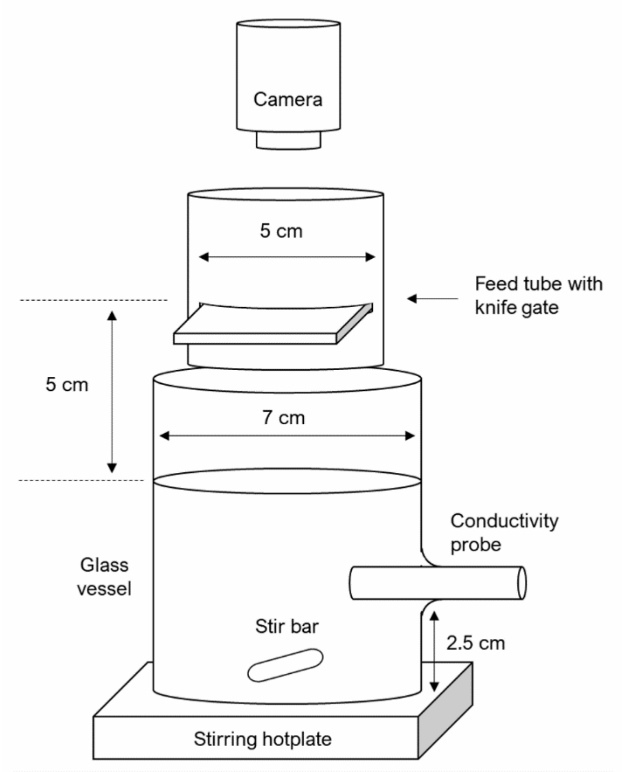

Figure 1. Reconstitution setup

The reconstitution values presented are the sinking time (t_{sink}) and dissolution time (t_{90}). Sinking time t_{sink} is the time it takes for the powder to become fully submerged into the liquid. The dissolution time t_{90} is the time to achieve 90% dissolution, i.e. the time required to reach 90% of the maximum conductivity value for each sample. The reconstitution experiments were performed ten times at each condition.

2.5 Scanning electron microscopy (SEM)

SEM was used for the characterization of the particle morphology and qualitative assessment of the coating. The instrument used was an InTouchScope from JEOL, Japan. Before SEM analysis, all samples were coated with gold using a sputter coater from Agar Scientific (UK) at 40 mA (25 mm sputtering distance, 12 s application time).

2.6 Particle size analysis

The volume-based particle size distributions of the different powders in this study were obtained using a Camsizer® XT by Retsch, Germany (dry dispersion module). A 180 kPa air dispersion pressure was applied for all powders except for agglomerated WMP, where the pressure was reduced to 60 kPa to minimize particle breakage. SMP was sieved prior to use so as to obtain a size distribution similar to non-agglomerated WMP, and the particle size distribution presented here is after sieving.

2.7 Free fat analysis

In order to quantify the free fat present in WMP, agglomerated WMP and SMP, a cold solvent fat extraction method was performed. Firstly, 2 g ± 0.2 g of powder were placed in a 100 ml screw-cap glass bottle. Next, 40 ml of n-heptane (HPLC grade, Sigma Aldrich, Germany) at room temperature were added. The bottle was closed tightly and was agitated at 60 ± 5 rpm for 5 minutes using a PSU-20i orbital shaker (Grant Instruments, UK). The powder and solvent were then separated by filtration (pre-pleated filter paper, 4 – 7 µm). Subsequently, 25 ml of the filtrate were transferred into an aluminum dish which was then placed on a heating plate at 110 ± 2°C for evaporation of the solvent. Following evaporation, the dishes were placed into a desiccator containing silica gel for 20 min.

2.8 Melting temperature of free fat

The free fat obtained by the extraction method described in §2.7 was subsequently used for DSC analysis. DSC measurements were performed using the DSC1 Star^{e} System (Mettler Toledo, Switzerland). The instrument was calibrated with an indium sample. For each measurement, 17 - 25 mg of sample were used (in a sealed aluminum crucible). Nitrogen was used as the purge gas.

The heating steps used to determine the melting point were the same as described in Kim et al. (2005). Firstly, the sample was brought to 70°C for 10 min so as to induce melting of all fat fractions. Afterwards, the sample was cooled down to -65°C at a rate of 10°C/min, followed by an isothermal step at -65°C for 10 min. Finally, the temperature was increased to 60°C at a rate of 5°C/min. Five measurements were performed, and the curve presented corresponds to the average values.

2.9 Dynamic viscosity

The dynamic viscosity of anhydrous milk fat (Emmi, Switzerland) was measured using a Malvern Kinexus Pro rheometer (Malvern, UK) with a cup and bob geometry (25 mm). Measurements were performed at 30, 35, 40, 50, 60 and 70°C. Before the measurement, the samples were heated in a water bath so as to reach the desired measurement temperature. The shear rate was varied from 1 to 100 s^{-1}, a range that spans the average shear rate values of interest for stirring during powder reconstitution in this study (see §2.4). The measurements at each temperature were performed in triplicate.

2.10 Statistical analysis

The statistical analysis was performed using the Real Statistics Resource Pack for Excel (Release 7.8). The data was subject to one-way analysis of variance (ANOVA) with Tukey's post-hoc test so as to compare all possible pairs of means and determine statistically significant differences between them. A 95% confidence level was selected, and a P-value of less than 0.05 was considered statistically significant. Prior to the analysis of variance, data normality was confirmed by the D'Agostino-Pearson test. All results are presented as the average ± 95% confidence intervals.

3 Results and discussion

3.1 Characterization of raw materials

SEM images of the raw materials are presented in Figure 2. WMP has a relatively smooth surface and consists of single particles or agglomerates of a few particles. For agglomerated WMP, relatively large agglomerates of irregular shapes can be observed. SMP has a shrivelled surface and is found in different shapes. Finally, fine particles can be observed in the case of micronized lactose powders, with no apparent differences between the two types.

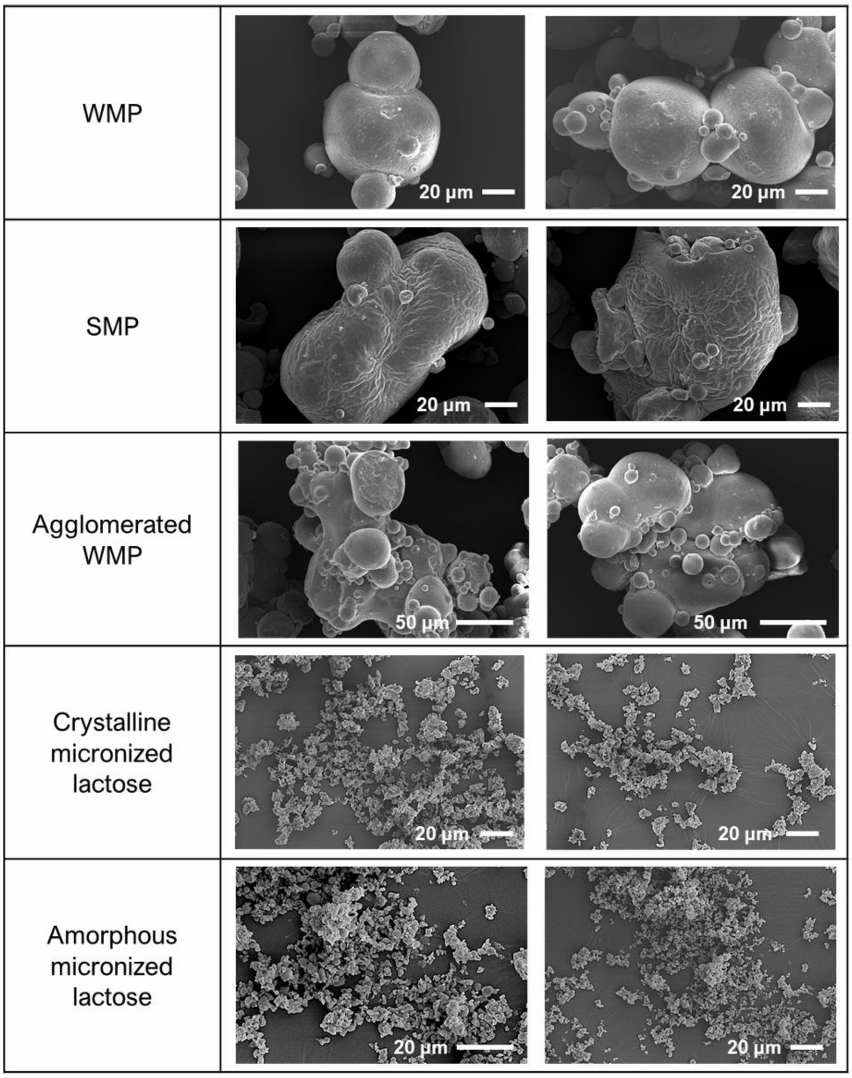

Figure 2. Scanning electron micrographs of raw materials

The d_{10}, d_{50} and d_{90} values, which represent the intercepts for 10%, 50% and 90% of the cumulative volume of the powders, are presented in Table 1. The non-agglomerated WMP has an average d_{50} of 80 µm. No significant difference in terms of d_{50} can be observed between WMP and SMP ($P < 0.05$). Agglomerated WMP has a d_{50} of 160 µm, which is double that of non-agglomerated WMP.

The free fat content of the different host powders used in this study is presented in Table 1. SMP has only traces of free fat (0.04%), while WMP (non-agglomerated and agglomerated) has a free fat content of 1 – 1.5%.

Table 1. Particle size distribution and free fat content of raw materials.

Property	WMP	SMP	Agglomerated WMP	Crystalline ML	Amorphous ML
d_{10} (µm)	31 ± 1^{a}	43 ± 1^{b}	62 ± 2^{c}	4 ± 0^{d}	3 ± 0^{e}
d_{50} (µm)	80 ± 6^{a}	72 ± 8^{a}	162 ± 6^{b}	6 ± 0^{c}	5 ± 0^{d}
d_{90} (µm)	153 ± 5^{a}	119 ± 8^{b}	352 ± 26^{c}	9 ± 0^{d}	6 ± 0^{e}
Free fat (g/100 g product)	1.1 ± 0.1^{a}	0.04 ± 0.02^{b}	1.4 ± 0.2^{c}	N/A	N/A

The errors represent 95% confidence intervals. Values followed by different superscript letters in the same row are significantly different ($P < 0.05$).
N/A: not applicable

3.2 Surface morphology of coated powders

SEM micrographs of the different coated powders are presented in Figure 3. A partial coating of the host particles with micronized lactose can be observed in all cases. No apparent differences can be spotted between the crystalline and amorphous coatings. A small difference in terms of coating distribution can only be observed for SMP, but it is not considered significant within the context of the current study.

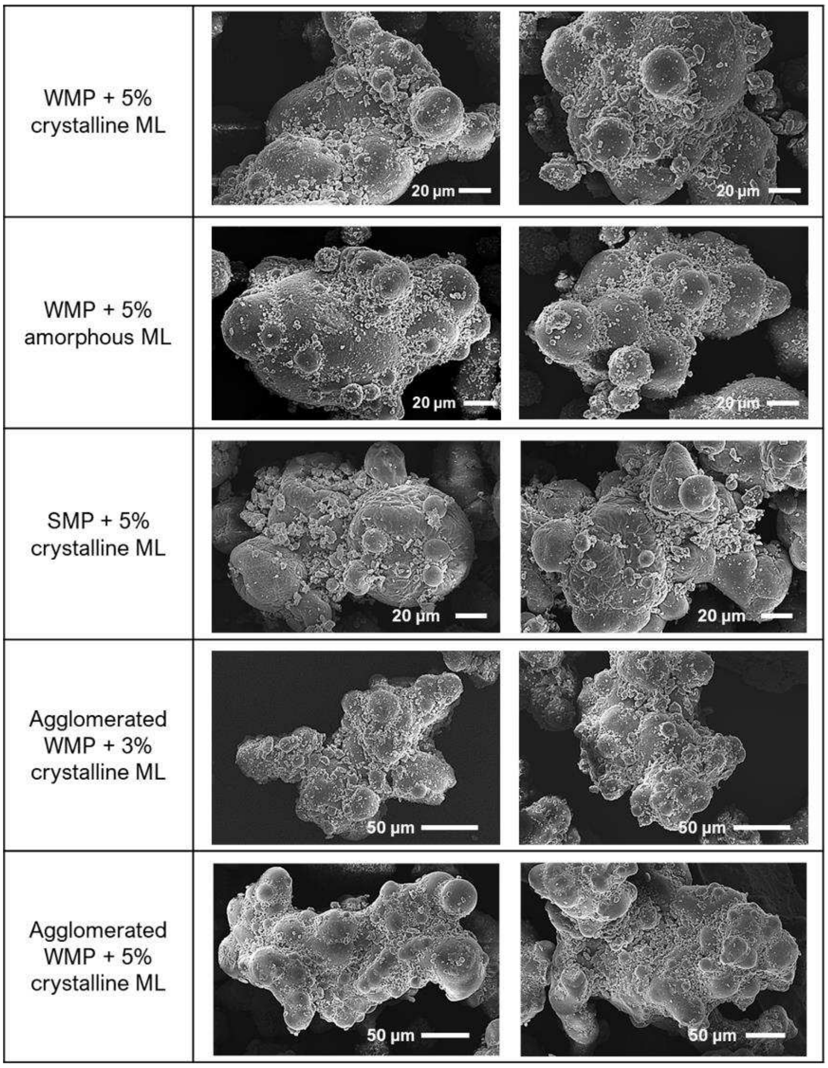

Figure 3. Scanning electron micrographs of coated powders

3.3 Effect of temperature and stirring rate on the reconstitution of coated WMP

The t_{sink} and t_{90} results of uncoated and coated WMP at the different temperatures and stirring rates are presented in Figure 4. At 4°C and 400 rpm, pure WMP is still floating on the surface of the liquid

6 h after the beginning of reconstitution, therefore no final t_{sink} and t_{90} values could be obtained (denoted by the empty marker).

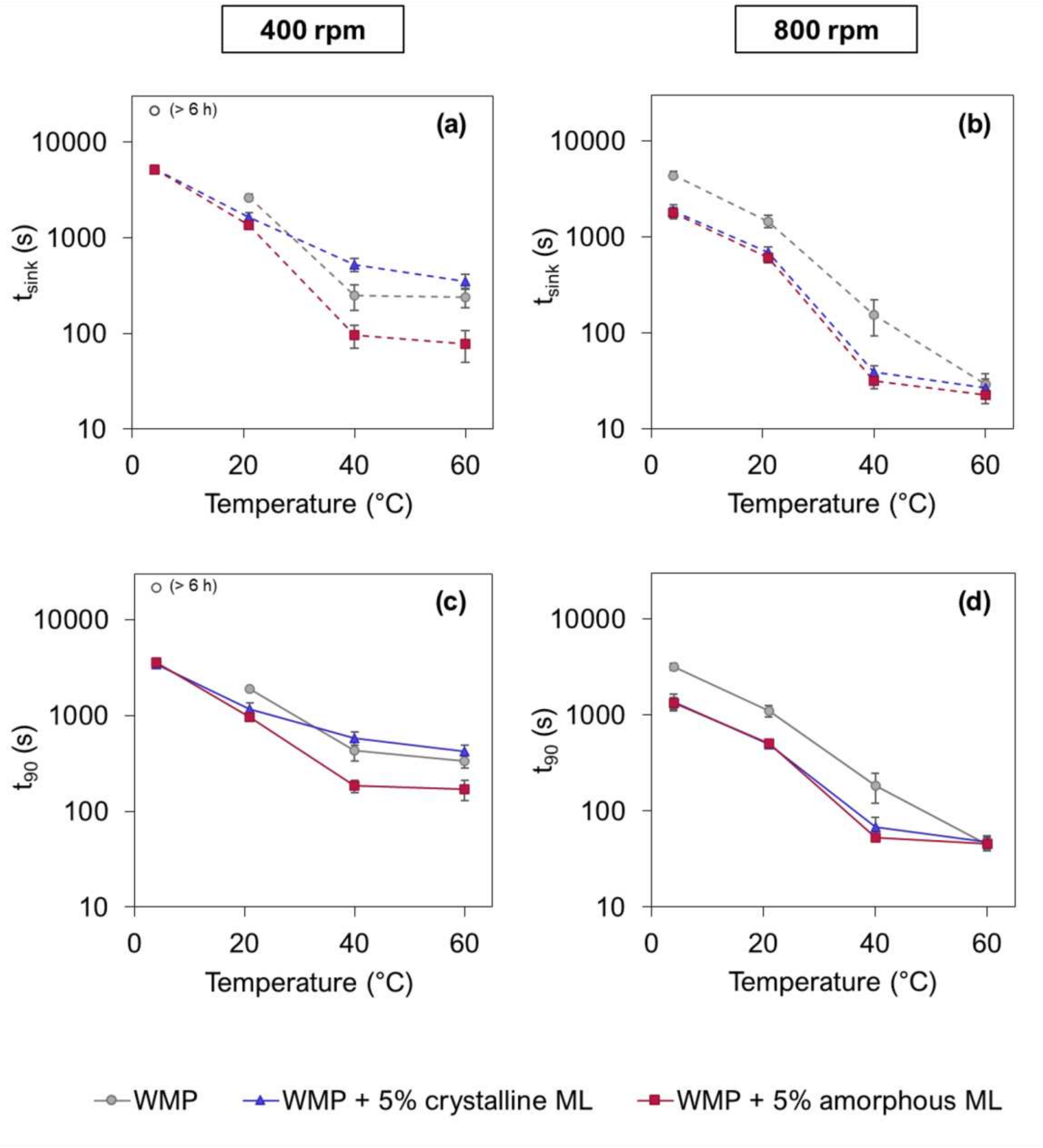

Figure 4. t_{sink} and t_{90} of WMP and WMP mixed with 5% (w/w) crystalline/amorphous micronized lactose (ML) at different temperatures and stirring rates: (a) t_{sink} at 400 rpm, (b) t_{sink} at 800 rpm, (c) t_{90} at 400 rpm, (d) t_{90} at 800 rpm. The empty marker in images (a) and (c) represents incomplete sinking (> 6 h floating).

Overall, increasing the temperature and stirring rate leads to a decrease in the sinking and dissolution times. The decrease in sinking time as a result of the increase in temperature is related to the partial or full melting of free fat (Kim et al., 2005; Mitchell et al., 2020). The decrease in sinking time by increasing the stirring rate can be explained by the greater drawdown due to increased turbulence and circulation velocity of the liquid (Khazam & Kresta, 2008; Mitchell et al., 2020). The decrease in dissolution time is linked to the faster sinking, as the submersion of powder enhances its exposure to the solvent. In addition, a higher temperature and stirring rate promote a faster mass transfer, thereby favoring the dissolution process (Richard et al., 2013).

The addition of micronized lactose (amorphous or crystalline) results in a significant decrease in the t_{sink} and t_{90} at 4°C and 21°C ($P < 0.05$), regardless of the stirring rate applied. The reconstitution improvement at these temperatures is associated with the wetting enhancement as a result of the hydrophilic micronized lactose coating. This mechanism is discussed in more depth in Angelopoulou et al. (2021).

At 40°C and 400 rpm, a peculiarity is observed: although the powder coated with amorphous micronized lactose sinks faster than WMP, crystalline micronized lactose has the opposite effect (see Figure 5 for a closer look).

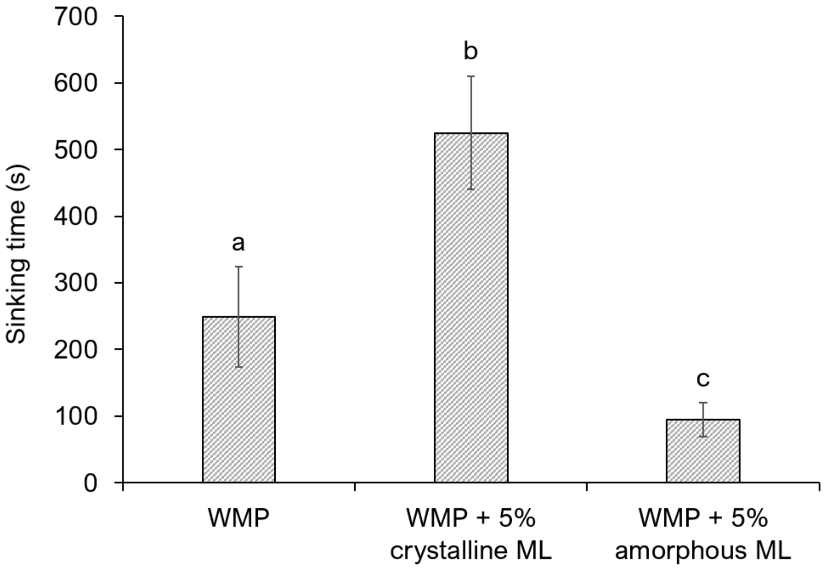

Figure 5. Sinking time of WMP and WMP + 5% ML (crystalline/amorphous) at 40°C/400 rpm. [a-c]Different letters above the bar plots indicate significant differences ($P < 0.05$).

At 60°C and 400 rpm, the powder that was coated with amorphous ML has a significantly shorter t_{sink} and t_{90} than pure WMP ($P < 0.05$). The opposite is observed in terms of t_{sink} for the powder coated with crystalline ML, while no significant differences appear between WMP and the crystalline ML-coated sample in terms of t_{90} ($P > 0.05$).

Increasing the stirring rate to 800 rpm at 40°C results in both coated powders having shorter t_{sink} and t_{90} than pure WMP ($P < 0.05$). At 60°C, a higher stirring rate leads to no significant differences in the sinking and dissolution times between the uncoated and coated powders ($P > 0.05$).

In order to explain the different effects of the crystalline and amorphous lactose coatings at 40/60°C and a low stirring rate, a series of experiments was performed, which is presented in the following paragraphs.

3.4 Influence of free fat

The free fat content of WMP in this study is 1.1% (see Table 1). SMP, on the other hand, has only traces of free fat (0.04%). For this reason, SMP was used as a host material so as to test the effect of free fat on the reconstitution of coated powders at 40°C and 400 rpm.

The sinking time of pure SMP and the SMP coated with 5% crystalline micronized lactose at 40°C/400 rpm is presented in Figure 6. No significant difference between the two powders can be observed in terms of sinking time. This suggests that the increase in the sinking time of WMP as a result of the crystalline micronized lactose coating at 40°C and 400 rpm (shown in Figure 5) can be associated with the presence of free fat (i.e. surface fat) in the host powder.

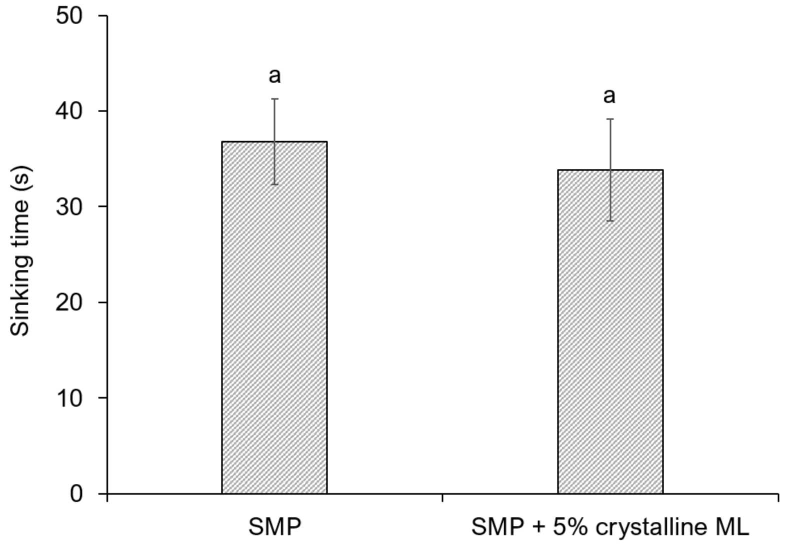

Figure 6. Sinking time of SMP and SMP + 5% crystalline ML at 40°C/400 rpm. [a]The same letter above the two bar plots indicates differences are not statistically significant ($P > 0.05$).

3.5 Influence of micronized lactose dissolution on the physical state and viscosity of surface fat

3.4.1 Dissolution enthalpy

Dissolution of micronized lactose is accompanied by a shift in the enthalpy of the system. According to Harjunen et al. (2004), dissolution of lactose in water at 25°C exhibits an enthalpy of -53.3 ± 2.7 $J\ g^{-1}$ if the lactose is amorphous (exothermic) or 54.2 ± 0.9 $J\ g^{-1}$ if the lactose is crystalline (endothermic). Similar values have also been reported by other studies (Hogan & Buckton, 2000; Listiohadi et al., 2009).

The effect of water temperature on the dissolution enthalpy at constant pressure can be estimated by Kirchhoff's equation (Atkins & Paula, 2011):

$$\Delta H_{T_2} = \Delta H_{T_1} + \int_{T_1}^{T_2} \Delta C_p\, dT \qquad (2)$$

where ΔH_{T_2} is the enthalpy of dissolution at the initial temperature T_2, and ΔH_{T_1} is the enthalpy of dissolution at the initial temperature T_1. ΔC_p is given by:

$$\Delta C_p = \bar{C}_p^{\infty} - C_{p_s} \qquad (3)$$

where $\bar{C}_p^{\infty}$ is the partial heat capacity of the solute (dissolved lactose), and C_{p_s} is the specific heat capacity of the solid material (solid lactose). Assuming heat capacities are independent of temperature, Kirchhoff's law can be expressed as (Atkins & Paula, 2013):

$$\Delta H_{T_2} = \Delta H_{T_1} + \Delta C_p (T_2 - T_1) \qquad (4)$$

According to Kawaizumi et al. (1981), ΔC_p of lactose in water is 198 $J\ K^{-1} mol^{-1}$. This is equal to ~ 0.58 $J\ °C^{-1} g^{-1}$. For a change in initial water temperature from 25°C to 40°C, the second component of Eq. 4 would be equal to 8.7 $J\ g^{-1}$. This is relatively small compared to the first component (i.e. enthalpy of dissolution at 25°C, ~ 55 $J\ g^{-1}$). Therefore, a change in initial temperature (within the range studied here) is not expected to have a major influence on the dissolution enthalpy of each material. This means that the differences observed between amorphous and crystalline lactose in terms of dissolution enthalpy are expected to be significant regardless of the water temperature before reconstitution.

3.4.2 Effect of dissolution enthalpy on local temperature

During reconstitution of the coated powders at a low stirring rate, a relatively large part of micronized lactose is expected to dissolve close to the liquid surface due to floating. This could lead to a localized thermal effect at the powder-liquid interface. To investigate this effect, a droplet of deionized water was placed on a micronized lactose bed and its temperature was monitored using thermal imaging. The initial temperature of the water droplet was 20°C (same as the powder and room temperature), so as to minimize evaporation and heat transfer from and to the environment.

The change in droplet temperature upon interaction with the micronized lactose bed is presented in Figure 7, both qualitatively (thermal images) and quantitatively (maximum droplet temperature). Deposition of the water droplet on the amorphous ML bed leads to an increase in temperature (~ 6.5°C), indicating an exothermic dissolution. Crystalline ML, on the other hand, results in a temperature decrease, thereby indicating an endothermic dissolution. The minimum droplet temperature upon deposition of the droplet on the crystalline ML bed was 18.6 ± 0.07°C, corresponding to a decrease of 1.4°C. The change in temperature upon deposition of the droplet was statistically significant for both micronized lactose physical states ($P < 0.05$).

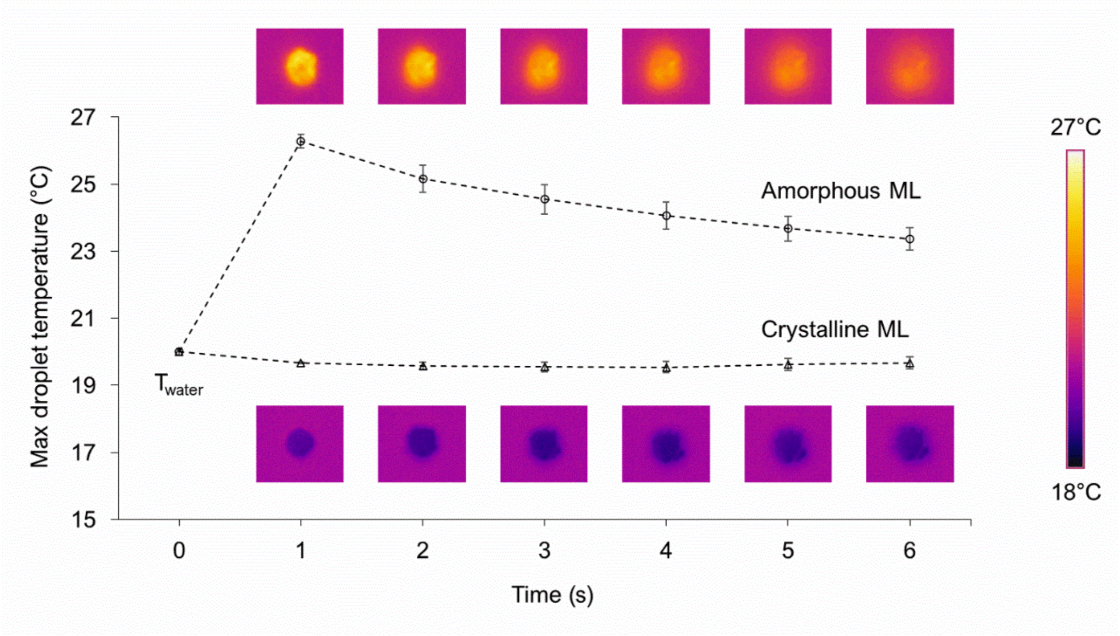

Figure 7. Maximum temperature of a water droplet added on a crystalline or amorphous ML powder bed as a function of time. t = 0 corresponds to the temperature of pure water before ML dissolution

3.4.3 Effect of dissolution enthalpy on the physical properties of surface fat

Thermal effects at the powder-liquid interface during reconstitution of coated powders could melt the surface fat, at least partially. To examine this effect, thermal imaging experiments were performed on layers of milk fat, either pure or coated with micronized lactose (crystalline/amorphous). The results obtained are presented in Figure 8 (optical and thermal images). The difference in terms of dissolution enthalpy between the two micronized lactose types is apparent in this case too. These images suggest that the dissolution of the coating material could have a significant effect on the temperature of surface fat during reconstitution of the coated powders.

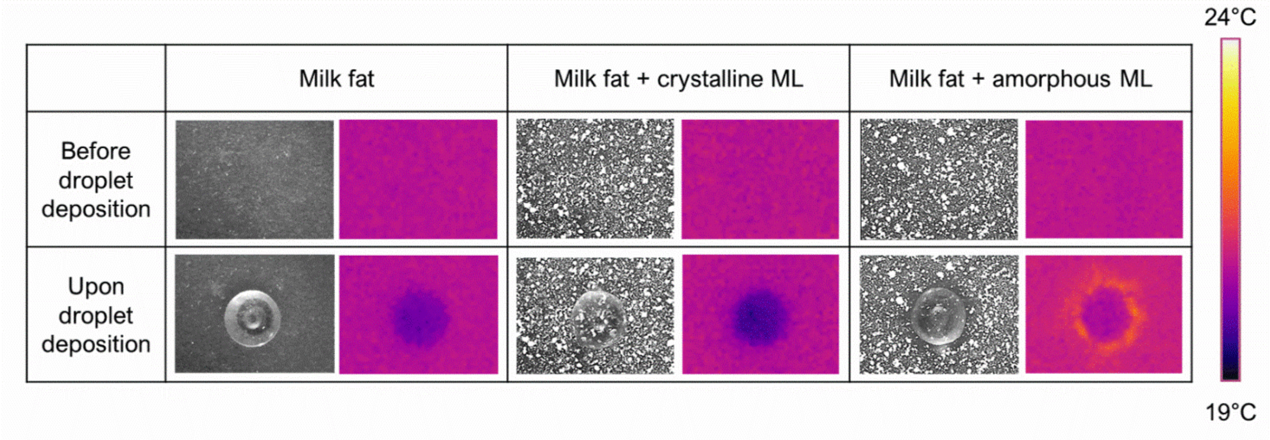

Figure 8. Temperature of a milk fat layer, either uncoated or coated with crystalline/amorphous ML, before and after deposition of a water droplet. In each column, the left side corresponds to optical images and the right side to thermal images

A shift in the temperature of surface fat during reconstitution can lead to changes in its physical state. Such an effect is expected to be particularly important during reconstitution at 40°C. As shown in Figure 9, melting of free fat starts at approximately -40°C and is completed at ~ 40°C. Therefore, 40°C is a threshold temperature above which all of the surface fat is expected to be liquid. A decrease in temperature due to the dissolution of crystalline micronized lactose during reconstitution at 40°C could hamper the complete melting of surface fat. It could, therefore, lead to presence of solid fat on the particle surface, which can be detrimental to powder wetting. This would explain the significant difference between amorphous and crystalline coatings in terms of reconstitution kinetics at 40°C (see Figure 4 and Figure 5). At the lower reconstitution temperatures tested in this study (i.e. 4/21°C), surface fat is expected to remain partially solid regardless of the dissolution enthalpy of the coating and substrate materials. Therefore, at these temperatures, dissolution enthalpy phenomena are not expected to have a significant effect on the wetting properties of the powder.

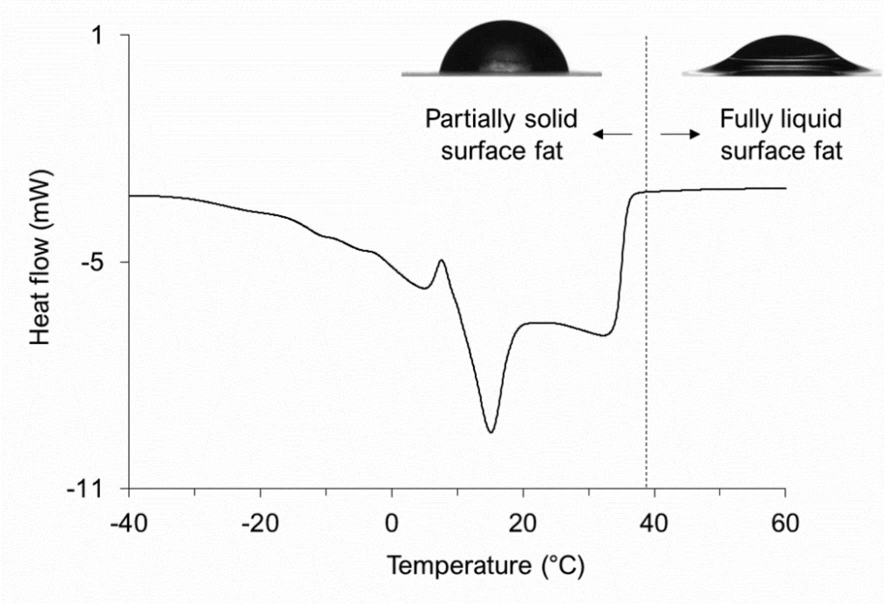

Figure 9. Differential scanning calorimetry of free fat. The embedded images represent water droplets deposited on a milk fat surface, either partially solid (left) or fully liquid (right)

Another property of free fat which could affect the reconstitution kinetics is the viscosity. As shown in Figure 10, the viscosity of milk fat is influenced by changes in temperature, with an increase in temperature leading to a decrease in viscosity. This effect is significant even above 40°C, where no changes in terms of physical state are expected to occur. Above 40°C, milk fat behaves like a Newtonian fluid. At 30°C and 35°C (where part of the fat is solid), a shear-thinning behavior is observed. Nevertheless, the differences in viscosity between the various temperatures tested here are significant at all shear rates applied.

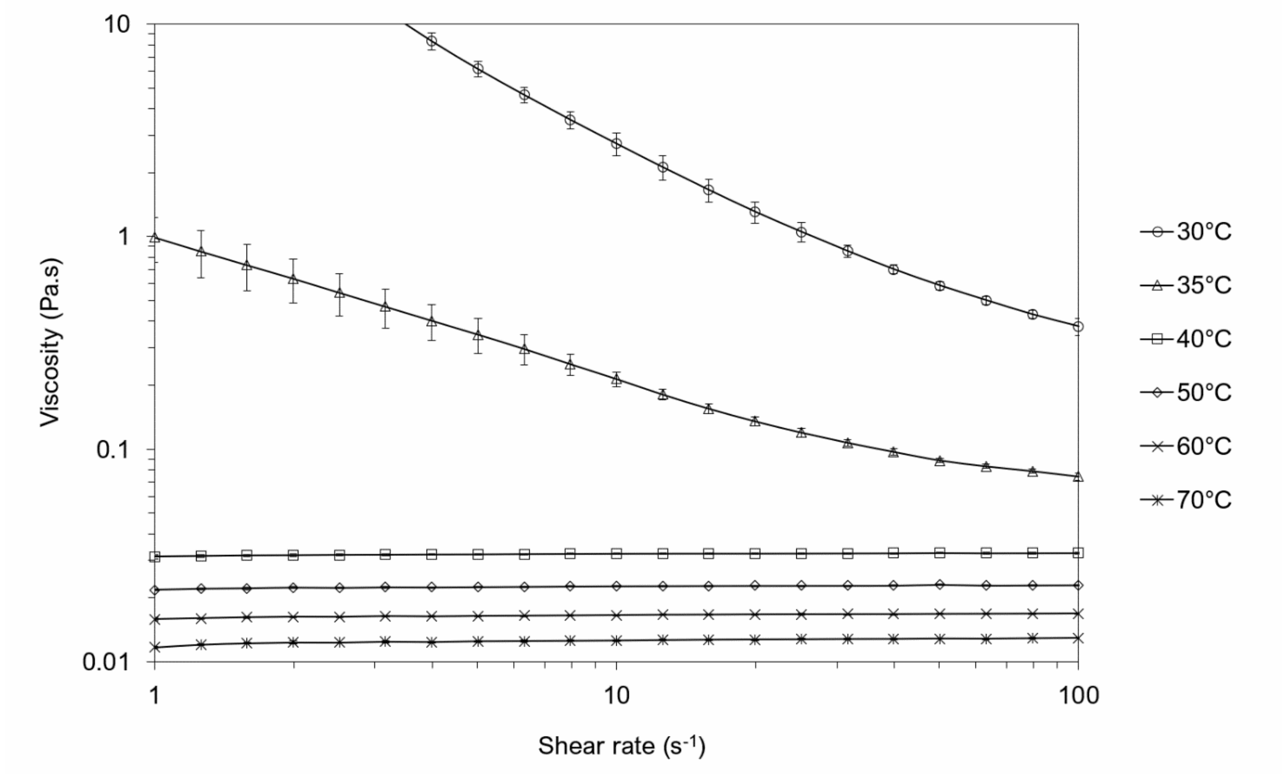

Figure 10. Dynamic viscosity of milk fat at different temperatures. The differences in viscosity between temperatures, at a given shear rate, are significantly different ($P < 0.05$).

Localized thermals effects due to the dissolution enthalpy of the coating material could have a significant effect on the viscosity of surface fat. More specifically, the exothermic effect of amorphous ML could lead to a decrease in the viscosity, while the dissolution of crystalline ML could have the opposite effect. At reconstitution temperatures ≥ 40°C, surface fat is expected to melt off of the particles and allow for water to rise into the inter- and intraparticle pores of the powder. A lower viscosity would make it easier for water to push the fat away from the liquid surface. The removal of surface fat can lead to contact line depinning (Bozon et al., 2021), and a faster capillary penetration and sinking. Such a mechanism could explain the significantly faster sinking of the powder coated with amorphous ML compared with pure WMP and the crystalline-coated powder at 40/60°C and 400 rpm (see Figure 4).

The differences in terms of reconstitution kinetics between the two coated powders at 40°C and 60°C are present only at a low stirring rate (Figure 4). An intense stirring of the liquid is expected to erase any localized thermal effects and minimize the impact of dissolution enthalpy.

Overall, the shortest reconstitution times were obtained at the highest temperature and stirring rate combination (60°C/800 rpm), with or without coating, and regardless of the physical state of the coating material.

3.6 Influence of powder mixing time

For the WMP and crystalline ML mixture, apart from the default dry mixing time, an additional experiment was performed in which the mixing time was varied (1, 3, 5 min). The sinking time was found to increase with the mixing time (Figure 11). One explanation could be the increase in coating uniformity due to better mixing. Another possibility is that a longer mixing leads to re-distribution of the fat on the particle surface. In the present study, dry mixing is performed at room temperature (~ 20°C). Figure 9 shows that at 20°C, part of the surface fat is liquid. During dry mixing of WMP with crystalline ML, the relatively hard and sharp crystalline ML particles may be pushing the (metastable) surface fat, thereby leading to changes in its distribution. This could have a negative impact on wetting and, combined with the endothermicity of dissolution of crystalline ML, could be causing additional delays in reconstitution.

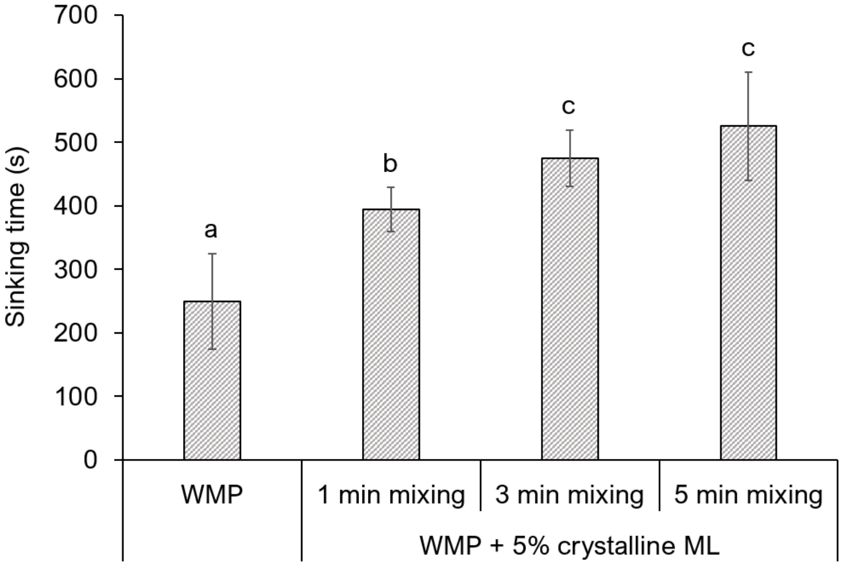

Figure 11. Sinking time of WMP and WMP + 5% crystalline ML prepared using different mixing times (1 min, 3 min and 5 min) at 40°C/400 rpm. [a-c]Different letters above the bar plots indicate significant differences ($P < 0.05$).

3.7 Influence of agglomeration

Apart from non-agglomerated WMP, agglomerated WMP was also used as a host powder. Agglomerated WMP was mixed with 3% and 5% (w/w) crystalline micronized lactose. 5% was the default concentration in the current study, while 3% corresponds to approximately the same micronized lactose surface coverage as the 5% concentration for the non-agglomerated WMP mixture (estimated by geometry calculations).

Figure 12 shows that the addition of crystalline micronized lactose on the surface of agglomerated WMP leads to a decrease in sinking time at 40°C and 400 rpm (statistically significant effect, $P < 0.05$). This effect is the opposite of what was observed for non-agglomerated WMP. This discrepancy could be explained by the different reconstitution regimes of the two host materials. The sinking of agglomerated WMP at 40°C/400 rpm occurs in less than 10 s (Figure 12), while the sinking time of non-agglomerated WMP at the same conditions is in the order of hundreds of seconds (see Figure 5). For agglomerated WMP, viscosity build-up phenomena are less pronounced, the gravity forces are higher, and sinking is no longer rate-limiting. Under these conditions, the impact of crystalline ML is different. This suggests that the crystalline ML coating can have a positive effect on the sinking of WMP at 40°C and 400 rpm, providing that WMP is agglomerated.

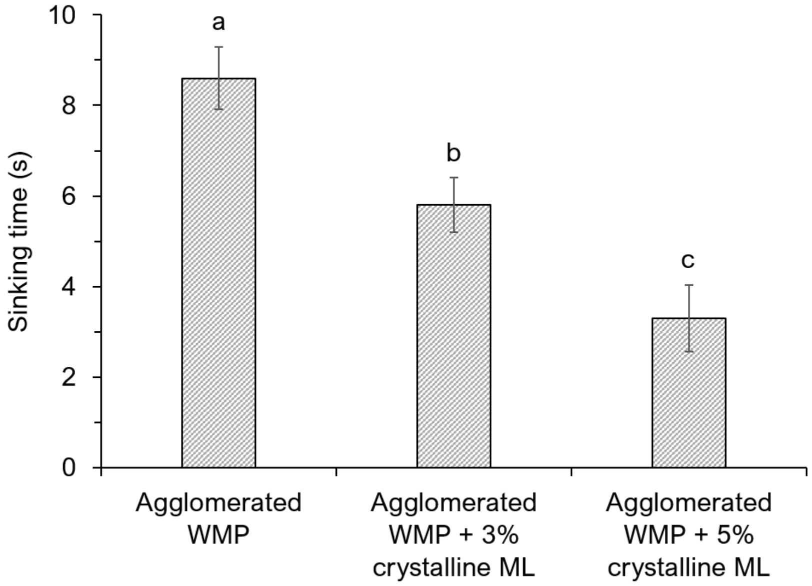

Figure 12. Sinking time of agglomerated WMP + crystalline ML (3% and 5%) at 40°C/400 rpm. [a-c]Different letters above the bar plots indicate significant differences ($P < 0.05$).

4 Conclusion

In the present study, we examined the effect of the physical solid state of a micronized lactose coating (crystalline/amorphous) on the reconstitution behavior of whole milk powder at different temperatures (4/21/40/60°C) and stirring rates (400/800 rpm).

It was demonstrated that both micronized lactose physical states have a positive impact on the sinking and overall reconstitution kinetics of whole milk powder if the temperature is relatively low (4/21°C), i.e. when part of the surface fat is solid. At temperatures above the melting point of surface fat (40/60°C) and 400 rpm, the amorphous micronized lactose coating accelerates sinking, while the crystalline coating has the opposite effect. This was primarily associated with differences in terms of dissolution enthalpy between the two lactose states. It was suggested that the dissolution of the coating material can cause a localized thermal effect and influence the physical properties of surface fat. No differences between the two lactose states were observed with increasing stirring rate, as the energy supplied is sufficient to erase any localized enthalpy effects. These differences are also overcome if agglomerated whole milk powder is used as the host material.

This study highlighted the importance of materials science in reconstitution research. The proposed component interactions provide a new perspective on reconstitution studies of fat-based dairy powders and should be considered when particle coating is performed for enhancing the reconstitution performance.

Acknowledgements

The authors would like to thank Teresa Kurtz and Delphine Pasche for their technical assistance.

Funding

This work was funded by the Société des Produits Nestlé, Vevey, Switzerland.

References

Alonso, M., Satoh, M., & Miyanami, K. (1989). Mechanism of the combined coating-mechanofusion processing of powders. *Powder Technology*, *59*(1), 45–52.

Angelopoulou, D., Meunier, V., Forny, L., Niederreiter, G., Palzer, S., & Salman, A. D. (2021). Particle surface design for enhanced reconstitution of fat-based food powders. *Powder Technology*, *393*, 397–404.

Atkins, P., & Paula, J. de. (2011). *Physical Chemistry for the Life Sciences*. W. H. Freeman and Company.

Atkins, P., & Paula, J. de. (2013). *Elements of Physical Chemistry*. W. H. Freeman and Company.

Bertrand, M., Parmentier, D., Lebaigue, O., Plasari, E., & Ducros, F. (2012). Mixing Study in an Unbaffled Stirred Precipitator Using LES Modelling. *International Journal of Chemical Engineering*, *2012*(ID 450491).

Bozon, A., Fries, L., Kammerhofer, J., Forny, L., Niederreiter, G., Palzer, S., & Salman, A. D. (2021). Effect of dissolution and partial hydrophobic coating on floating of crystalline particles. *Powder Technology*, *392*, 264–277.

Clark, Z., Paterson, A. H. J., Joe, R., & Mcleod, J. S. (2016). Amorphous lactose crystallisation kinetics. *International Dairy Journal*, *56*(Supplement C), 22–28.

Foerster, M., Gengenbach, T., Woo, M. W., & Selomulya, C. (2016). The impact of atomization on the surface composition of spray-dried milk droplets. *Colloids and Surfaces B: Biointerfaces*, *140*(Supplement C), 460–471.

Forny, L., Marabi, A., & Palzer, S. (2011). Wetting, disintegration and dissolution of agglomerated water soluble powders. *Powder Technology*, *206*(1), 72–78.

Gaiani, C., Ehrhardt, J. J., Scher, J., Hardy, J., Desobry, S., & Banon, S. (2006). Surface composition of dairy powders observed by X-ray photoelectron spectroscopy and effects on their rehydration properties. *Colloids and Surfaces B: Biointerfaces*, *49*(1), 71–78.

Harjunen, P., Lehto, V.-P., Koivisto, M., Levonen, E., Paronen, P., & Järvinen, K. (2004). Determination of Amorphous Content of Lactose Samples by Solution Calorimetry. *Drug Development and Industrial Pharmacy*, *30*(8), 809–815.

Hogan, S. E., & Buckton, G. (2000). The quantification of small degrees of disorder in lactose using solution calorimetry. *International Journal of Pharmaceutics*, *207*(1), 57–64.

Huppertz, T., & Gazi, I. (2016). Lactose in dairy ingredients: Effect on processing and storage stability1. *Journal of Dairy Science*, *99*(8), 6842–6851.

Kawaizumi, F., Nishio, N., Nomura, H., & Miyahara, Y. (1981). Heat-capacity measurements of aqueous solutions of mono-, di-, and tri-saccharides using an isoperibol twin calorimeter. *The Journal of Chemical Thermodynamics*, *13*(1), 89–98.

Khazam, O., & Kresta, S. M. (2008). Mechanisms of solids drawdown in stirred tanks. *The Canadian Journal of Chemical Engineering*, *86*(4), 622–634.

Kim, E. H.-J., Chen, X. D., & Pearce, D. (2005). Melting characteristics of fat present on the surface of industrial spray-dried dairy powders. *Colloids and Surfaces B: Biointerfaces*, *42*(1), 1–8.

Kim, E. H.-J., Chen, X. D., & Pearce, D. (2009). Surface composition of industrial spray-dried milk powders. 1. Development of surface composition during manufacture. *Journal of Food Engineering*, *94*(2), 163–168.

Listiohadi, Y., Arthur Hourigan, J., Robert Walter Sleigh, & John Steele, R. (2009). Thermal analysis of amorphous lactose and α-lactose monohydrate. *Dairy Science & Technology*, *89*(1), 43–67.

Marabi, A., Mayor, G., Raemy, A., Bauwens, I., Claude, J., Burbidge, A. S., Wallach, R., & Saguy, I. S. (2007). Solution calorimetry: A novel perspective into the dissolution process of food powders. *Food Research International*, *40*(10), 1286–1298.

McNaught, A. D., & Wilkinson, A. (1997). *Compendium of Chemical Terminology: IUPAC Recommendations*. Wiley.

Metzner, A. B., & Otto, R. E. (1957). Agitation of non-Newtonian fluids. *AIChE Journal*, *3*(1), 3–10.

Mitchell, W. R., Forny, L., Althaus, T., Niederreiter, G., Palzer, S., Hounslow, M. J., & Salman, A. D. (2019). Surface tension-driven effects in the reconstitution of food powders. *Chemical Engineering Research and Design*, *146*, 464–469.

Mitchell, W. R., Forny, L., Althaus, T., Niederreiter, G., Palzer, S., Hounslow, M. J., & Salman, A. D. (2020). Tracking of powder lump formation and dispersion with the use of FBRM technology and video recordings. *Powder Technology*, *367*, 10–19.

Mitchell, W. R., Forny, L., Althaus, T. O., Niederreiter, G., Palzer, S., Hounslow, M. J., & Salman, A. D. (2015). Mapping the rate-limiting regimes of food powder reconstitution in a standard mixing vessel. *Powder Technology*, *270*, 520–527.

Murrieta-Pazos, I., Gaiani, C., Galet, L., & Scher, J. (2012). Composition gradient from surface to core in dairy powders: Agglomeration effect. *Food Hydrocolloids*, *26*(1), 149–158.

Nijdam, J. J., & Langrish, T. A. G. (2006). The effect of surface composition on the functional properties of milk powders. *Journal of Food Engineering*, *77*(4), 919–925.

Obermayer, D., Damm, M., & Kappe, C. O. (2013). Design and evaluation of improved magnetic stir bars for single-mode microwave reactors. *Organic & Biomolecular Chemistry*, *11*(30), 4949–4956.

Pfeffer, R., Dave, R. N., Wei, D., & Ramlakhan, M. (2001). Synthesis of engineered particulates with tailored properties using dry particle coating. *Powder Technology*, *117*(1), 40–67.

Richard, B., Le Page, J. F., Schuck, P., Andre, C., Jeantet, R., & Delaplace, G. (2013). Towards a better control of dairy powder rehydration processes. *International Dairy Journal*, *31*(1), 18–28.

Roos, Y. H. (2010). Glass Transition Temperature and Its Relevance in Food Processing. *Annual Review of Food Science and Technology*, *1*(1), 469–496.

Saleh, K., & Guigon, P. (2007). *Chapter 7 Coating and encapsulation processes in powder technology* (A. D. Salman, M. J. Hounslow, & J. P. K. Seville, Eds.; Vol. 11). Elsevier.

Wu, J., Graham, L. J., & Mehidi, N. N. (2006). Estimation of agitator flow shear rate. *AIChE Journal*, *52*(7), 2323–2332.